

# Geochemistry of Extremely Alkaline (pH > 12) Ground Water in Slag-Fill Aquifers

by George S. Roadcap<sup>1,2</sup>, Walton R. Kelly<sup>3</sup>, and Craig M. Bethke<sup>2</sup>

---

## Abstract

Extremely alkaline ground water has been found underneath many shuttered steel mills and slag dumps and has been an impediment to the cleanup and economic redevelopment of these sites because little is known about the geochemistry. A large number of these sites occur in the Lake Calumet region of Chicago, Illinois, where large-scale infilling of the wetlands with steel slag has created an aquifer with pH values as high as 12.8. To understand the geochemistry of the alkaline ground water system, we analyzed samples of ground water and the associated slag and weathering products from four sites. We also considered several potential remediation schemes to lower the pH and toxicity of the water. The principal cause of the alkaline conditions is the weathering of calcium silicates within the slag. The resulting ground water at most of the sites is dominated by  $\text{Ca}^{2+}$  and  $\text{OH}^-$  in equilibrium with  $\text{Ca}(\text{OH})_2$ . Where the alkaline ground water discharges in springs, atmospheric  $\text{CO}_2$  dissolves into the water and thick layers of calcite form. Iron, manganese, and other metals in the metallic portion of the slag have corroded to form more stable low-temperature oxides and sulfides and have not accumulated in large concentrations in the ground water. Calcite precipitated at the springs is rich in a number of heavy metals, suggesting that metals can move through the system as particulate matter. Air sparging appears to be an effective remediation strategy for reducing the toxicity of discharging alkaline water.

---

## Introduction

Extremely alkaline ground water has not been extensively studied because it is observed only rarely in natural water, and then only in distinctive geological settings, such as thermal springs or ultramafic terrains (Hem 1985). In a small area of northern Jordan, for example, pH in wells and adits is as high as 12.5, apparently due to the hydration of portlandite formed by the subterranean combustion of organic matter in a bituminous marl formation (Khoury et al. 1985). The pH also can exceed 10 in hypersaline evaporative lakes, such as Mono Lake in California or lakes in the Rift Valley of eastern Africa. Human activities can also produce high pH water.

Reaction with fly ash leachates commonly produces pH values in excess of 10 (Mattigod et al. 1990), and the dissolution of concrete can drive pH above 12 (Berner 1988).

Human activities have also produced the extremely alkaline ground water found around steel mills and slag dumps. The wetlands of the Lake Calumet region of southeast Chicago (87°36'W, 41°41'N), along the southern margin of Lake Michigan (Figure 1), provide a number of good examples of extremely alkaline systems. The widespread wetland complexes in this low-lying region have been used intensively since the 1880s to dispose of a variety of industrial wastes (Colton 1985). Steel production, a major industry in the region, has profoundly affected the landscape and environment. The slag wastes produced by the steel mills were used as fill to convert the extensive wetlands into usable industrial and residential property. The slags are primarily high-temperature calcium silicate minerals and can contain as much as 50% metallic iron (Fe) and manganese (Mn), along with other steel additives such as chromium (Cr), molybdenum (Mo), and vanadium (V). Lithologic logs from the area indicate that slag is the most common fill type. However, significant amounts of other potentially harmful solid

---

<sup>1</sup>Corresponding author: Illinois State Water Survey, 2204 South Griffith Drive, Champaign, IL 61820; Roadcap@uiuc.edu

<sup>2</sup>Department of Geology, University of Illinois, 1301 West Green Street, Urbana, IL 61801.

<sup>3</sup>Illinois State Water Survey, 2204 South Griffith Drive, Champaign, IL 61820.

Received August 2004, accepted December 2004.

Copyright © 2005 National Ground Water Association.

doi: 10.1111/j.1745-6584.2005.00060.x

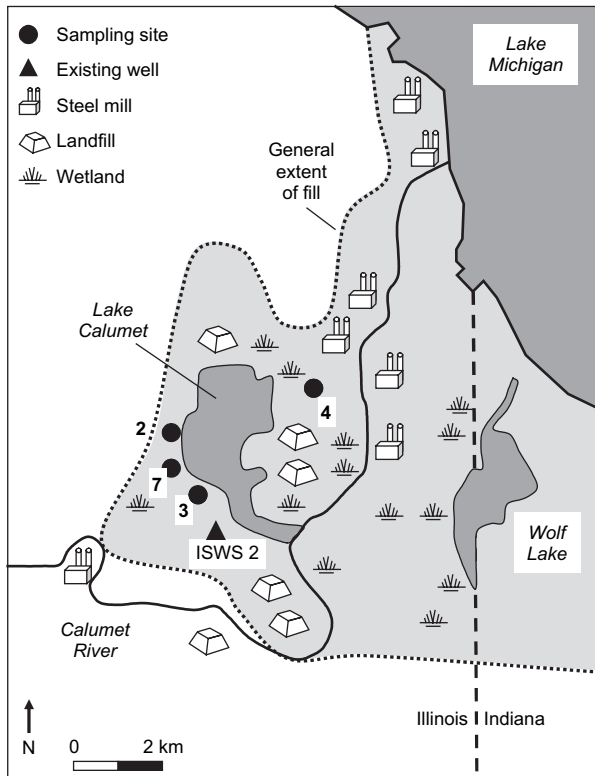


**Figure 1. Location of sampling sites in the Lake Calumet region and generalized distribution of fill material. Both active and inactive slag-producing steel mills are shown.**

wastes also were used, including fly ash, solid industrial wastes, demolition debris, and household trash (Colton 1985). A significant amount of dredged material from the deepening and channelization of the Calumet River system was also used as fill (Colton 1985). Kay et al. (1996) estimate that 600 million m<sup>3</sup> of fill was dumped over a 150-km<sup>2</sup> area in southeast Chicago and northwest Indiana. The fill was placed on top of up to 6 m of unconsolidated beach sands and silts that, along with the fill, form a shallow unconfined aquifer that overlies ~20 m of low-permeability glacial till.

The fill, especially the vast amount of reactive steel slag, has profoundly affected the ground water quality of the surficial aquifer in the region. As a result, ground water sampled from many monitoring wells in the region is contaminated (IEPA 1986; Cravens and Zahn 1990; Fenelon and Watson 1993; Roadcap and Kelly 1994; Duwelius et al. 1996; Bayless et al. 1998). In terms of major ion chemistry and heavy metal content, ground water here is among the most degraded of any shallow aquifer in Illinois. Typical problems include extremely alkaline pH (>12), high total dissolved solids (TDS) (>5000 mg/L), and high concentrations of iron (>20 mg/L) and ammonia (>50 mg/L). High levels of barium, chromium, and manganese and moderate concentrations of 17 other metals, including lead, mercury, arsenic, and lithium, have also been found (Roadcap and Kelly 1994). Some of the observed contamination may have originated from sources other than fill, such as leakage from municipal landfills, spills at hazardous waste-handling facilities or along roads, road-salt runoff, and illegal dumping. The

horizontal and vertical variation of the water chemistry in the shallow aquifer is complex due to the truckload-by-truckload way the fill material was dumped.

The purpose of this study is to better understand the geochemical processes occurring in alkaline ground water and spring water. From a chemical perspective, a better understanding is needed of the reactions occurring within the slag fill and how these affect the movement of metals through the system. This understanding has important implications for how the environment could potentially support bacteria and how the water chemistry there may affect aquatic life in downstream wetlands. To these ends, we sampled the slag, ground water, and weathering products at four locations. We then tested potential remediation schemes for mitigating the toxicity of the discharging alkaline water.

### Sampling Sites

We identified potential locations for collecting highly alkaline ground water using the data from existing monitoring wells reported in Roadcap and Kelly (1994) and additional field inspections. On the basis of these results, we excavated a test pit in an area of slag fill and located seeps where active precipitation of calcite was occurring on plants and debris in the wetlands. We did not use existing monitoring wells for further study because fresh solid samples were not available from them. In addition, many of the wells were screened across multiple layers and produced mixtures of fluids of differing composition. We chose two springs (sites 2 and 7), one shallow pond (site 3), and one test pit (site 4) for further geochemical study (Figure 1). At each site, we sampled water and the calcite precipitate that is actively being deposited. At sites 3 and 4, we collected samples of the steel slag that makes up the aquifer matrix. The property upgradient of sites 2 and 7 was inaccessible for constructing test pits or monitoring wells from which the fill samples could be collected; however, boring logs in the area report a variety of slags up to 3 m in thickness. The topography of the surrounding fill areas at each site is flat, and the water table is generally within 1 m of the surface.

The site 2 spring is in a line of springs that discharge into a vegetated roadside ditch. Water from this site has a dark red color due to large amounts of humic compounds, which are observed to flocculate when enough acid is added to a sample to drop the pH below 2. A chemical plant that produces a variety of volatile organic compounds is located on a property upgradient of the springs.

Site 3 is a small isolated pond in the middle of a multi-hectare expanse of former wetlands that have been filled with steel slag. The pond is fed by diffuse ground water inflow and is generally <0.5 m deep. The pond has been observed to go dry for extended periods. Since the pond was created in the early 1990s, a layer of calcite precipitate up to 10 cm in thickness has accumulated on the bottom. The land surrounding the site is largely unvegetated and has never been developed.

The setting of site 4 is similar to that of site 3. The 2-m deep test pit here was excavated to collect the solid

samples for this study and to assess the feasibility of recycling the entire steel slag pile for its iron content. Ground water was sampled as it entered the sides of the test pit while the pit was actively dewatered. A sample of the calcite precipitate was collected at a downgradient spring 40 m away where the local ground water discharges into a large wetland complex.

Site 7 is an ephemeral spring located 300 m south of site 2, in a different branch of the same drainage system. The upgradient land use at site 7, which includes an at-grade garbage landfill, a junkyard, and a former metal smelter/foundry site with metal-contaminated soil, differs from that at site 2. At the time the spring was sampled, two overland flows mixed with the spring discharge as it moved down the ditch. Samples of the water, filtered as described subsequently, and sediment were collected along the discharge path of the spring. An unfiltered sample was also collected for a total metals analysis.

## Field and Laboratory Methods

All sampling and analytical procedures followed a quality assurance project plan approved by a quality assurance manager at the U.S. EPA. Conductivity, pH, temperature, and dissolved oxygen were measured in situ using a calibrated Hydrolab multiprobe. The pH probe was calibrated with pH 7 and pH 10 buffers and checked against a saturated calcium hydroxide ( $\text{Ca}(\text{OH})_2$ ) solution (pH = 12.43 at 25°C). Samples for determination of dissolved anion, cation, nonvolatile organic carbon (NVOC), and ammonia ( $\text{NH}_3\text{-N}$ ) concentrations were filtered in the field using a peristaltic pump and Geotech 0.45 micron high-capacity filters. The cation samples were preserved with nitric acid to a pH <2, and the NVOC and  $\text{NH}_3\text{-N}$  samples were preserved with sulfuric acid. Because of their high alkalinities, some samples required significant amounts of acid, up to 5% by volume. Samples were transported and stored on ice.

Chemical analyses were performed at the Illinois State Water Survey laboratory, which was certified by the Illinois Environmental Protection Agency. The laboratory used ion chromatography (IC) for the anions (U.S. EPA Method 300.0), inductively coupled plasma (ICP) atomic emission spectrometry for the cations (U.S. EPA Method 200.7), colorimetry for  $\text{NH}_3\text{-N}$  (Standard Method 4500), and persulfate/ultraviolet oxidation for NVOC (U.S. EPA Method 415.2). The method detection limits varied among samples because different dilution rates were needed to insure that the highly concentrated ions fell within the working range of the IC and ICP atomic emission spectrometry instruments. For the dissolved heavy metals detected at all four sites, the micromolar detection limits from the site 7 analyses are aluminum 1.6, barium 0.029, chromium 0.17, copper 0.079, strontium 0.068, vanadium 0.16, and zinc 0.12. Data precision was assessed by the analysis of duplicate field samples, and data accuracy was assessed by the collection of field blanks and laboratory fortified matrices (LFM). All of the analyses passed the quality assurance guidelines except for Zn analyses in the duplicate and LFM samples where the

relative errors were 62% and 86%, respectively. The Zn data are used here with caution. We characterized the minerals present in the different weathering horizons in the site 4 test pit using x-ray diffraction (XRD). Representative solid samples were crushed to a powder in a ball mill and mounted on a slide. The XRD analyses were performed using a Rigaku Rotoflex diffractometer and the Jade<sup>®</sup> peak analysis software.

For geochemical modeling, we used the React reaction path model within The Geochemist's Workbench<sup>®</sup> software package (Bethke 2002). Using the analytical and field data from the fluid at each site, React calculated the equilibrium distribution of aqueous species, the saturation state with respect to minerals, and the fugacity of dissolved gases. The activity coefficients were calculated using the Debye-Hückel equation with the B-dot extension. The thermodynamic database compiled by Lawrence Livermore National Laboratory was used, with the addition of metallic iron.

Water and sediment samples from site 3 were subjected to laboratory experiments designed to evaluate four remediation strategies aimed at lowering the pH: (1) sparging with carbon dioxide ( $\text{CO}_2$ ); (2) sparging with air; (3) adding hydrochloric acid (HCl); and (4) adding locally available, crushed dolomite aggregate. In each case, 1-L flasks were prepared containing 900 mL of site water and 100 g of precipitate from the top of the sediment column. For the air and  $\text{CO}_2$  experiments, the water was sparged with a glass gas dispersion tube at a constant rate until the pH stabilized. For the acid addition experiment, 0.1 M HCl was titrated into a continuously stirred flask until the pH stabilized due to the dissolution of the sediment. For the dolomite-addition experiment, 35 g of fine-grained crushed dolomite that had been passed through a 0.5-mm sieve was added to a continuously stirred flask. Samples were collected from the experiments for Microtox<sup>®</sup> toxicity-screening tests (Azure 2000) to determine the extent to which the remediation schemes might improve the quality of the aquatic habitat. The Microtox test uses the colorimetric response of the luminescent bacteria *Vibrio fischeri* to measure the decrease in metabolic activity (increase in mortality) caused by toxic substances in a water sample.

## Results and Discussion

### Source Material and Weathering Products

The slag dumped throughout the region is mainly iron slag, the byproduct of producing pig iron from ore material, and steel slag, the byproduct of producing steel from pig iron. Iron slag is formed in the blast furnace from the limestone or dolomite added to the molten iron ore to remove silica and other impurities. A sample of recent iron slag from the USX mill in Gary, Indiana, was composed of the calcium-magnesium silicate mineral akermanite ( $\text{Ca}_2\text{MgSi}_2\text{O}_7$ ) and contained little to no iron (Vythoukaskas 1997). Because a blast furnace operates continuously and produces one product, iron slag is rather uniform in composition. In contrast, the mineralogy and metal content of steel slag varies greatly from day to day,

depending upon the alloy being made. Steel slag generally is composed of large amounts of metal mixed with calcium silicate minerals. The chemical composition as well as the physical properties, such as color, grain size, and density, of the steel slag dumped throughout the region varies dramatically. The steel slags at sites 3 and 4 are a gray, magnetic, poorly cemented, poorly sorted, silt to gravel-sized material.

Total digestion and analysis of samples from sites 3 and 4 (Table 1) show the slag to be comprised largely of Fe (up to 26 wt%), Ca, Mg, Mn, and Si. Slag from site 4 contains a significant amount of Zn, whereas site 3 slag contains little Zn but abundant Al. Heavy metal composition also varies among the sites, with site 3 slag having large amounts ( $\geq 400$  mg/kg) of Cr, Cu, Ti, and V, and site 4 slag containing significant ( $\geq 700$  mg/kg) Pb and Ti.

In the shallow subsurface, the slag reacts with water and air to add solutes to the ground water and produce weathering products. Vythoulkas (1997) examined the mineral and metal composition of steel slag dating from the 1920s, taken from gravel-sized samples collected during the construction of monitoring well ISWS 2 (Roadcap and Kelly 1994; Figure 1). The unweathered cores of the slag contained roughly 50 wt% high-temperature, glassy to very fine-grained, calcium silicate minerals and 50 wt% metal oxides and steel droplets. The metals often occur as dendrites embedded in silicate minerals. As this

material was exposed to the environment, it reacted to form a weathering rind composed primarily of calcite ( $\text{CaCO}_3$ ), dolomite ( $\text{CaMg}(\text{CO}_3)_2$ ), quartz ( $\text{SiO}_2$ ), and pyrite ( $\text{FeS}_2$ ).

On a larger scale, the geochemical evolution of the steel slag is apparent in the test pit excavated at site 4. The pit exposed 2 m of steel slag overlying the native sand deposit (Figure 2). The upper 0.7 m contained layers of iron-stained weathered slag interspersed within loosely cemented, gray unweathered slag. The weathering occurred preferentially in coarser layers, where high permeability and porosity allowed air and water to circulate freely. A 0.6-m thick zone of gray unweathered slag underlies the interspersed zone but remains above the water table. The lower 0.7 m of the slag is a second weathered zone that is generally below the water table and contains iron staining throughout. Additional weathering products are accumulating as a layer of chemical precipitate up to 10 cm in thickness where the site 4 ground water discharges into the adjacent wetland. XRD analyses show the precipitate to be calcite.

The XRD analyses of samples from site 4 show an increase in the diversity of crystalline alteration products in the weathered zones (Figure 2). The dominant mineral in the unweathered slag is wustite ( $\text{FeO}$ ). The iron minerals magnetite ( $\text{Fe}_3\text{O}_4$ ), mackinawite ( $\text{FeS}$ ), and srebrodolskite ( $\text{Ca}_2\text{Fe}_2\text{O}_5$ ) are found as weathering products

**Table 1**  
**Cation Composition of Slags and Calcite Precipitates in the Sediment**

	Site 3		Sites 4		Site 7	
	Slag	Sediment	Slag	Sediment	Sediment (0 m)	Sediment (6 m)
Major elements (g/kg)						
Aluminum	10	2.7	3.5	1.3	6.1	13
Calcium	>100	>100	84	~470	>100	>100
Iron	110	2.2	260	2.5	46	96
Magnesium	36	1.8	120	14	20	16
Manganese	32	0.088	15	0.41	0.71	1.3
Silicon	40	5.3	~40	3.7	14	24
Zinc	0.081	0.026	11	0.060	4.3	6.1
Minor elements (mg/kg)						
Arsenic	16	<16	79	<12	<22	<22
Barium	270	150	78	170	520	1600
Boron	150	7.1	110	34	92	110
Cadmium	23	<2.0	27	0.91	30	50
Chromium	1000	12	92	15	45	330
Cobalt	33	<1.4	29	2.5	44	25
Copper	400	8.3	79	12	190	630
Lead	44	<9.5	770	33	1100	4100
Lithium	20	4	4.1	<1.8	14	17
Molybdenum	140	<2.9	120	<1.8	<3.9	16
Nickel	11	3.6	49	6.2	31	76
Phosphorous	2800	<42	400	330	960	3700
Potassium	1700	580	<3.4	2600	1200	3200
Sodium	<12	<12	1000	410	810	1700
Sulfur	890	380	1000	1800	4300	8700
Strontium	150	280	42	730	450	241
Tin	<8.9	<8.9	22	4.1	150	570
Titanium	3900	570	700	1200	99	940
Vanadium	720	33	86	57	8.4	77

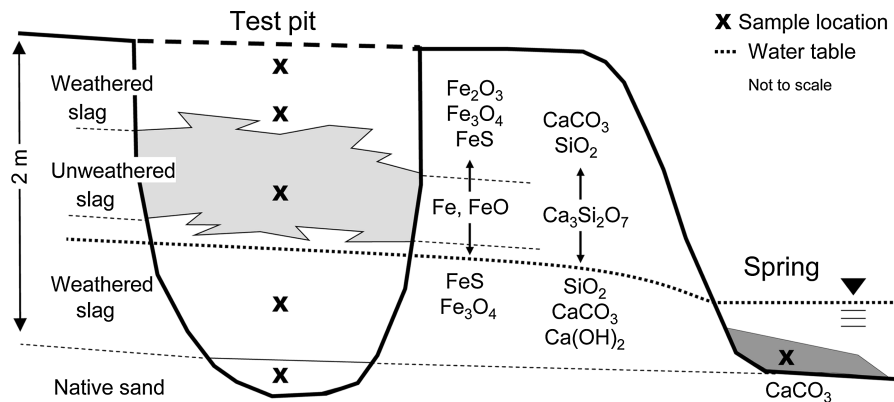


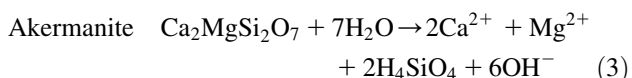
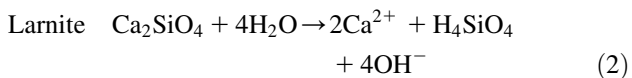
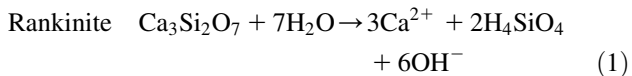
**Figure 2. Generalized cross section and location of sampling sites for XRD analysis at site 4. Labels show the slag mineralogy and location of additional weathering products in the different weathering zones.**

in the lower zone. In the upper zone, magnetite and mackinawite appear along with the ferric iron minerals maghemite ( $\gamma\text{-Fe}_2\text{O}_3$ ), hematite ( $\text{Fe}_2\text{O}_3$ ), and magnesioferrite ( $\text{MgFe}_2\text{O}_4$ ). Hausmannite ( $\text{Mn}_3\text{O}_4$ ) and hauerite ( $\text{MnS}_2$ ) were found in both weathered zones, and wurtzite ( $\text{ZnS}$ ) was found in the upper zone. The calcium silicate portion of the slag is composed of rankinite ( $\text{Ca}_3\text{Si}_2\text{O}_7$ ), larnite ( $\text{Ca}_2\text{SiO}_4$ ), and wollastonite ( $\text{CaSiO}_3$ ). Tridymite ( $\text{SiO}_2$ ) and calcite ( $\text{CaCO}_3$ ) are present in both weathered zones, and portlandite ( $\text{Ca}(\text{OH})_2$ ) is present in the lower zone. Tridymite is the stable form of quartz at the high-temperature and low-pressure conditions of a steel furnace and is commonly found in refractory bricks (Zoltai and Stout 1984). Minerals not readily detectable with XRD, such as amorphous silica and amorphous iron oxyhydroxides, may also be present.

The minerals found in the underlying native Holocene sand at site 4 include quartz, dolomite, and minrecordite ( $\text{CaZn}(\text{CO}_3)_2$ ). Secondary calcite, dolomite, iron oxides, minrecordite, and clay minerals along with pitted primary quartz fragments were found in the native sand immediately beneath a slag pile at a site in Indiana (Bayless et al. 1998; Bayless and Schultz 2003). At this site, the secondary precipitation and dissolution may indicate a shift in mineral saturation states as alkaline ground water migrates from the slag into the sand aquifer where pH is near-neutral.

### Weathering Reactions

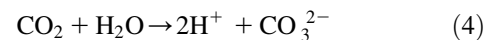
The calcium silicates within the slag react with the ground water by the following proposed reactions:



Each of these reactions releases calcium ions and consumes protons, creating a Ca-OH ground water. At

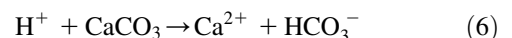
$\text{Ca}(\text{OH})_2$  saturation, a Ca-OH solution has a temperature-dependent pH ranging from 13.36 at  $0^\circ\text{C}$  to 10.71 at  $95^\circ\text{C}$ ; at  $25^\circ\text{C}$ , the pH is 12.43. We used a reaction path model to simulate the dissolution of  $1\text{ cm}^3$  of larnite in dilute rain water in a closed system over a typical range of laboratory and ground water temperatures. The models predicted a pH of 12.4 at  $25^\circ\text{C}$  and 13.0 at  $8^\circ\text{C}$ . The model also predicted a  $\text{CO}_2$  fugacity of  $10^{-13}$ , the equilibrium  $\text{pCO}_2$  between  $\text{CaCO}_3$  and  $\text{Ca}(\text{OH})_2$  in a  $\text{CaO-CO}_2\text{-H}_2\text{O}$  system at  $25^\circ\text{C}$  (Langmuir 1997).

The presence of calcite in the weathering products suggests a source of carbonate that is external to the slag. The source is likely a combination of  $\text{CO}_2$  diffusing from the atmosphere,  $\text{HCO}_3^-$  and  $\text{H}_2\text{CO}_3$  carried in by infiltrating precipitation, and  $\text{HCO}_3^-$  derived from the underlying sands and soils. The added carbonate reacts with the site water to form  $\text{CO}_3^{2-}$ , the dominant carbonate species above about pH 10.3, and two protons, lowering pH. The  $\text{CO}_3^{2-}$  reacts with  $\text{Ca}^{2+}$  in the ground water to form calcite:



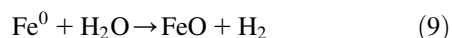
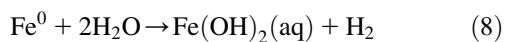
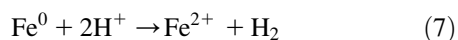
Where the ground water is rich in calcium, it has the potential to form considerable amounts of calcite if exposed to atmospheric  $\text{CO}_2$ . In a geochemical model of the site 4 water, increasing the  $\text{CO}_2$  fugacity from the equilibrium value of  $3 \times 10^{-13}$  to the atmospheric value of  $3 \times 10^{-4}$  causes calcite to precipitate and the pH to decrease 4 units, to 8.3.

This behavior contrasts with that of a ground water with near-neutral pH. In this case, adding  $\text{CO}_2$  causes calcite to dissolve. The  $\text{CO}_2$  contributes both  $\text{H}^+$  and  $\text{HCO}_3^-$  to the water, but since there are fewer  $\text{H}^+$  than  $\text{HCO}_3^-$  ions in solution initially, the relative concentration of the former increases more than that of the latter. As a result, the reaction for calcite dissolution is driven forward:



Metallic Fe, Mn, Zn, Al, and trace metals such as Cr and V are released from the slag as it weathers. The

metals oxidize through corrosion reactions that increase pH and produce dihydrogen (H<sub>2</sub>):



In a geochemical model of the reaction between metallic iron and rain water under reducing conditions (i.e., the near absence of molecular O<sub>2</sub>), the hydrogen ions available are consumed rapidly and the pH increases to ~11.5, according to Reaction 7. After this point, H<sub>2</sub>O becomes the principal oxidant and aqueous ferrous hydroxide is formed (Reaction 8); the final pH is 11.9. If in the model minerals are allowed to precipitate, crystalline FeO forms and the pH remains near-neutral at 8.1 because H<sup>+</sup> is not consumed. The oxides found in the weathered slag are similar to the layers of increasingly oxidized iron minerals, from FeO to Fe<sub>2</sub>O<sub>3</sub>, observed as corrosion products on iron pipes (Cornell and Schwertmann 1996).

### Ground Water Chemistry

The water chemistry at these high-pH sites varied broadly from the dilute aerobic Ca-OH water at site 3 to the more saline, organic-rich anaerobic Na-SO<sub>4</sub> water at site 2 (Table 2). These differences in chemistry arise from variations in the composition of the slag matrix as well as the effects of other waste materials that may have been dumped along with the slag. The TDS of water from sites 2, 4, and 7 varied from 1900 to 5100 mg/kg (Table 2), which is within the range observed in nearby monitoring wells (Roadcap and Kelly 1994).

The pH and alkalinity of the ground water at site 4 appear to be controlled by the temperature-dependent buffering reaction of a saturated Ca(OH)<sub>2</sub> solution. The pH measurements over the course of a year (Figure 3) varied by 0.5 pH units and paralleled the trend of the saturated calcium hydroxide solution. Considering the accuracy of the field probe (±0.2 pH units), the offset of 0.1 to 0.2 pH units between the field measurements and the saturated Ca(OH)<sub>2</sub> solution is probably not significant. At a pH of 12.5, a change of 0.1 pH units dramatically changes the OH<sup>-</sup> concentration. To achieve a charge balance in the site 4 water, the OH<sup>-</sup> concentration needs to be increased from 24 to 52.6 mmolal, which corresponds to an increase in pH of 0.12 units. This result further suggests that the pH value measured in the field is slightly lower than the actual pH.

The pH measurements from site 2, which contains a Na-SO<sub>4</sub> rather than a Ca-OH ground water, fell significantly below the pH curve of the saturated calcium hydroxide solution and correlated poorly with temperature compared to those from site 4 (Figure 3). The lower pH values probably were due to the fluid's high carbonate concentration of 11.5 mmolal, as determined by alkalinity titration. Reaction between HCO<sub>3</sub><sup>-</sup> and CO<sub>3</sub><sup>2-</sup>, rather than buffering by Ca(OH)<sub>2</sub>, appears to control pH at this site.

The relatively high alkalinity values measured for the samples do not necessarily suggest that the water contains high concentrations of carbonate. In solutions with pH values >11, OH<sup>-</sup> can account for a significant portion of a fluid's alkalinity. To calculate the concentrations of OH<sup>-</sup> and CO<sub>3</sub><sup>2-</sup> at each site, the alkalinity titrations were simulated with a reaction path model; results are listed in Table 2. At sites 4 and 7, the alkalinity was almost exclusively from OH<sup>-</sup>. Because the solutions at these sites had high concentrations of Ca<sup>2+</sup>, any CO<sub>3</sub><sup>2-</sup> entering the systems causes calcite to become supersaturated and precipitate, according to Reaction 5. At site 2, CO<sub>3</sub><sup>2-</sup> accounts for 70% of the alkalinity and OH<sup>-</sup> makes up 30%. In contrast to the other sites, the precipitation of calcite here was limited by the availability of Ca<sup>2+</sup>.

The dissolved oxygen concentrations indicate that redox conditions at the high-pH sites ranged from anoxic at site 2 to fully oxygenated at site 3. Varying redox conditions might be expected in the aquifer because the types of waste materials used as fill can differ significantly in chemical and physical properties. Materials such as slag and municipal garbage tend to be very reducing. Degradation of organic material in the underlying till, sand, and buried soil generates CH<sub>4</sub> that diffuses up into the saturated slag, adding additional reducing power. Reduced organic matter also infiltrates into the slag from the land surface or the adjacent wetlands. Because the aquifer is near the surface, atmospheric O<sub>2</sub> can diffuse into the system. Therefore, the ground water system, including solids, is rich in reduced species (e.g., H<sub>2</sub>, CH<sub>4</sub>, metallic Fe, NH<sub>4</sub><sup>+</sup>) and oxidized species (e.g., O<sub>2</sub>, SO<sub>4</sub><sup>2-</sup>, ferric oxides, NO<sub>3</sub><sup>-</sup>) that can serve, respectively, as electron donors and acceptors. The zonation of redox conditions is complex and likely varies over different scales. It is also possible that flow into a spring or a well comprises coalescing water of dissimilar chemistries and redox states.

Eh values calculated from analytical data for various half reactions differed from each other and the field-measured Eh values (Figure 4), confirming redox disequilibria at the sites. Platinum Eh electrodes, as in the frequently cited paper by Lindberg and Runnells (1984), do not respond uniformly to the redox potentials generated by the different redox couples. As such, field-measured Eh reflects only in a qualitative sense the relatively oxidizing conditions at site 3 and the more reducing conditions at sites 2, 4, and 7. Both the reduced (as NH<sub>3</sub> above pH 9.4) and oxidized (NO<sub>3</sub><sup>-</sup>) forms of nitrogen occurred at sites 3, 4, and 7. Nitrate dominated in the oxic water from site 3, whereas NH<sub>3</sub> dominated in the anoxic site 4 water (Table 2). No dissolved oxygen measurement was available for site 7, but the predominance of nitrogen as NO<sub>3</sub><sup>-</sup> suggests the water was relatively oxic. As expected, Eh values computed from the NH<sub>3</sub> and NO<sub>3</sub><sup>-</sup> concentrations are close to 0V, corresponding to the equal-activity point for the two species (Figure 4). Similarly, Eh values of around -0.58V can be computed for the SO<sub>4</sub><sup>2-</sup>/FeS redox couple linking the dissolved SO<sub>4</sub><sup>2-</sup> and the observed secondary sulfide minerals at site 4.

**Table 2**  
**Chemical Analysis of Ground Water**

Site	2	3	4	7	7 <sup>1</sup>
pH	12.2	11.2	12.5	12.2	
Temperature (°C)	13.6	14.5	17	8.7	
Eh (V)	-0.27	0.25	-0.045	-0.24	
TDS (mg/kg)	5100	170	2400	1900	
Dissolved oxygen (mmolal)	<0.01	0.55	<0.12		
NVOC (mmolal C)	6.8	0.33	0.92	1.83	
Major ions (mmolal)					
Calcium	0.27	0.82	27	18	18
Magnesium	0.010	0.005	<0.001	<0.002	0.20
Potassium	0.61	0.69	1.2	0.59	0.59
Sodium	78	0.57	2.2	2.5	2.7
Chloride	3.4	0.093	2.1	7.9	
Sulfate	20	0.14	0.055	0.22	
Alkalinity (CaCO <sub>3</sub> )	19	1.2	27	16	
Modeled OH <sup>-</sup>	12	1.6	53	33	
Modeled CO <sub>3</sub> <sup>2-</sup>	13	0.33	0.58	<0.02	
Minor ions (μmolal)					
Ammonia	210	15	360	39	
Nitrate/nitrite	— <sup>2</sup>	47	52	150	
Fluoride	53	53	270	240	
Phosphate	— <sup>2</sup>	<1.3	0.10	0.57	
Aluminum	30	12	5.2	2.1	20
Arsenic	9.5	<1.7	<0.53	<1.7	<3.3
Barium	0.30	0.23	2.7	2.2	2.0
Boron	69	<3.7	8.3	30	31
Cadmium	<0.14	<0.14	<0.04	<0.14	<0.10
Chromium	0.46	0.31	0.83	0.35	0.40
Cobalt	<0.19	<0.19	0.32	<0.19	<0.12
Copper	0.54	0.52	0.36	0.55	0.60
Iron	9.1	<0.16	0.7	<0.16	15
Lead	<0.36	<0.36	0.14	<0.36	<0.30
Lithium	6.1	4.9	<0.58	6.6	7.9
Manganese	0.09	<0.05	0.15	<0.05	0.55
Molybdenum	0.49	<0.24	0.06	0.39	0.27
Nickel	<0.41	<0.41	0.85	<0.41	0.65
Silicon	2700	61	<7.8	22	36
Strontium	0.64	1.5	37	9.5	9.6
Tin	<0.59	<0.59	<0.34	<0.59	<0.93
Titanium	0.17	<0.10	0.73	<0.10	0.21
Vanadium	2.6	0.20	0.10	0.29	0.27
Zinc	34	8.9	3.5	3.5	9.6

<sup>1</sup>Unfiltered.  
<sup>2</sup>“—” indicates no result, excess interference from sulfate on IC.

### Distribution of Metals

Understanding the fate in alkaline ground water of the major metals and steel additives found in slag, such as Cr, Cu, and V, is important to understanding the controls on the water's quality and toxicity. At high pH, Fe and Mn released from the weathering slag are likely to precipitate as oxide, hydroxide, sulfide, or carbonate minerals. With the exception of the 9.1 μmolal Fe<sup>2+</sup> at site 2, the concentrations of dissolved Fe and Mn observed in the ground water were <0.7 μmolal. Formation of new Fe and Mn solids in the weathered slag was confirmed by XRD analyses, which detected the oxides hematite (Fe<sub>2</sub>O<sub>3</sub>) and hausmannite (Mn<sub>3</sub>O<sub>4</sub>) and the sulfides mackinawite (FeS) and hauerite (MnS<sub>2</sub>). Which secondary

minerals form at the site likely depends on local redox conditions, the availability of sulfide, and the kinetic rates of the reactions. The relative lack of Fe and Mn (<11% by oxide weight) in the weathering rind analyzed by Vythoukcas (1997) suggests that at his site these metals are mobile over distances of at least a few centimeters.

Three of the other major components in the slag, Al, Zn, and Si, are soluble at high pH. Al and Zn were observed at concentrations between 2 and 60 μmolal in the water at each site; Si varied from below detection limits at site 4 to 2.7 mmolal at site 2 (Table 2). These metals were also present in particulate matter, as indicated by the analysis of the unfiltered sample from site 7. The total concentrations of Al, Zn, and Si in this sample were 10, 3,

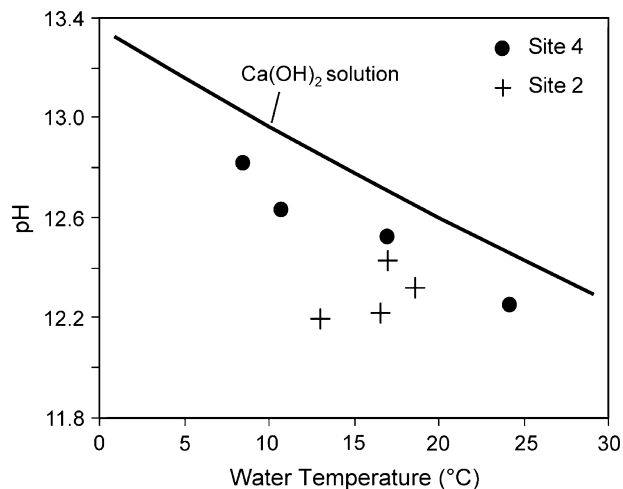
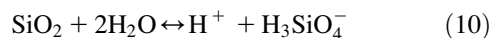


Figure 3. pH variation with water temperature at sites 2 and 4.

and 2 times higher, respectively, than the dissolved concentrations. In high-pH solutions, aluminum minerals such as gibbsite ( $\text{Al}(\text{OH})_3$ ), kaolinite ( $\text{Al}_2\text{Si}_2\text{O}_5(\text{OH})_4$ ), and feldspars are undersaturated and were not found within the weathered slag. Clay minerals were found precipitating within the sand below the slag at an Indiana site (Bayless and Schultz 2003). Wurtzite ( $\text{ZnS}$ ) forms in the presence of sulfide ions and was observed by XRD analysis of the weathered slag at site 4.

The presence of quartz in the slag weathering rinds examined by Vythoulkas (1997) suggests that silica crystallizes in place as the slag dissolves. Geochemical models and a remediation experiment discussed subsequently provide evidence that the water at each site is undersaturated with respect to quartz. When quartz-containing dolomite aggregate was added to a sample of site 3 water,

the concentration of dissolved silica slowly increased and the pH slowly decreased by the dissolution reaction:



In the top of the sand underlying the slag at the Indiana site, Bayless and Schultz (2003) found pitted quartz fragments, also an indication of quartz dissolution by high-pH water. Therefore, the secondary quartz may slowly dissolve over time after its initial crystallization in the weathering rind.

Even though the concentrations of trace metals in the slag are up to 0.7 wt%, the concentrations of trace metals in the water generally occurred near or below the detection limits. Of the trace metals listed in Tables 1 and 2, barium (Ba), strontium (Sr), and titanium (Ti) are thermodynamically insoluble at high pH (Brookins 1988). Boron (B), tin (Sn), lead (Pb), and vanadium (V) are soluble at high pH. Chromium (Cr) is soluble under oxidizing conditions but forms insoluble  $\text{Cr}_2\text{O}_3$  under reducing conditions. Arsenic (As), cadmium (Cd), cobalt (Co), copper (Cu), molybdenum (Mo), and nickel (Ni) are also soluble under oxidizing conditions but form insoluble sulfides under reducing conditions. Many of these metals may have been removed from solution by coprecipitation with and sorption to other minerals, such as iron oxides and calcite (Bayless and Schultz 2003). Metals that can substitute for Fe in goethite and hematite include Al, Cd, Cr, Co, Cu, Pb, Mn, Ni, Ti, V, and Zn (Cornell and Schwertmann 1996).

The substantial concentration of metals in the calcite precipitates suggests that metals move through the water as colloidal-sized particulate matter as evidenced by the analysis of the unfiltered sample from site 7 (Table 2). Fe, Mg, and Mn were observed in the unfiltered sample, but were not detected after the sample was passed through a standard 0.45- $\mu\text{m}$  filter. The concentrations of Al, Si, and Zn also were reduced substantially by the filter. The apparent importance of the suspended load in transporting metals may be due in large part to a lack of natural filtering in the macropores that form the springs at sites 2, 4, and 7.

From a mass balance perspective, the trace metal concentrations in the slag are a poor predictor of their concentration in the calcite precipitate. Of the 15 trace metals found in the slag at site 4, As, Li, and Mo were not detected in the precipitate, whereas B, Cd, Cr, Co, Cu, Pb, Ni, Sb, and V appeared in concentrations that varied anywhere from 1.5 to 30 times less than in the slag (Table 1). The concentrations of Cd, Cr, Cu, Pb, Ni, and Zn in the calcite exceed (U.S. EPA 1996) sediment toxicity thresholds for fresh water. Three of the more insoluble metals, Ba, Sr, and Ti, were more concentrated in the precipitate at site 4 than in the slag.

The observation that many of the trace metals appeared in the precipitate at lower concentrations than in the slag may be due in part to the mass of carbonate anions in the precipitate because the slag has no anions in the metallic phases and only oxygen as an anion in the silicate phases. The slag samples analyzed, furthermore, may not be representative of the slag's bulk composition. Most of the effect, however, is likely thermodynamic,

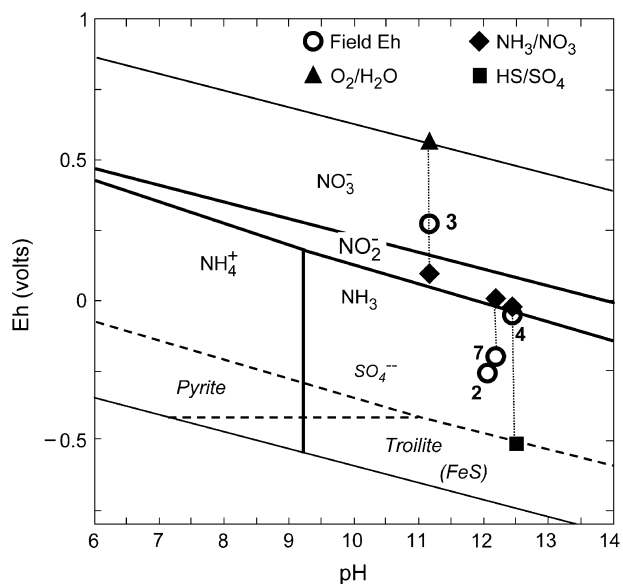


Figure 4. Eh-pH diagram showing field-measured Eh values, calculated Eh values for the  $\text{O}_2(\text{aq})/\text{H}_2\text{O}$  and  $\text{NO}_3^-/\text{NH}_3$  redox couples, and an estimated Eh for the  $\text{SO}_4^{2-}/\text{FeS}$  redox couple. Vertical dotted lines connect points from the same site.

reflecting the compatibility of the metals in the calcite crystal structure.

### Mixing of Alkaline Ground Water with Surface Water

The evolution of water chemistry at site 7, where the spring discharge mixes in contact with the atmosphere with two surface water inflows, reveals details of how the calcite precipitate forms. On the day the site was sampled, the spring flow mixed with an ~50% larger inflow of surface runoff at a point 1 m downstream of the spring (Figure 5). The pH dropped from 12.2 to 11.8 as the runoff, which had a pH of 7.4 and was likely saturated with atmospheric CO<sub>2</sub>, mixed into the CO<sub>3</sub><sup>2-</sup> depleted spring water. After the mixing zone, pH continued to drop along a 1-m long zone of turbulent flow. Three meters downstream of the spring, a second surface stream discharged into the ditch from a culvert at a flow rate roughly equal to the combined flow of the spring and the first surface inflow. The second inflow had a pH of 8.6 and was also likely saturated with atmospheric CO<sub>2</sub>. By the time the water had traveled 6 m from the spring, the pH in the water had decreased to 7.7.

The spring water reacted actively as it discharged, as evidenced by the buildup of calcite precipitate several centimeters thick along the bottom of the ditch. The spring had a high Ca<sup>2+</sup> concentration (18 mmolal) that decreased along the flowpath as pH dropped (Figure 6). Carbonate ions, formed from the introduction of CO<sub>2</sub> from the surface water and the atmosphere, reacted with the Ca<sup>2+</sup> to form calcite (Reactions 4 and 5). A geochemical model of the spring water indicates that the initial CO<sub>2</sub> fugacity was  $<1 \times 10^{-11}$  atm, compared to the atmospheric value of  $3 \times 10^{-4}$  atm. An antithetical process is commonly observed where a spring of near-neutral pH discharges from a limestone aquifer. In this case, it is the degassing of CO<sub>2</sub>, not its dissolution, that causes calcite to precipitate (Hem 1985).

By the time the pH in the ditch had fallen to 9.0, the concentration of dissolved calcium had dropped 82%, to

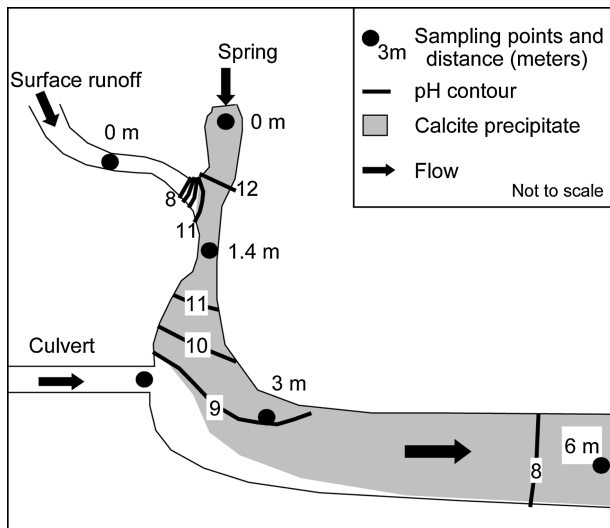


**Figure 5. Map of spring and surface drainage at site 7. Contours show the distribution of pH, and shading shows where calcite precipitates.**

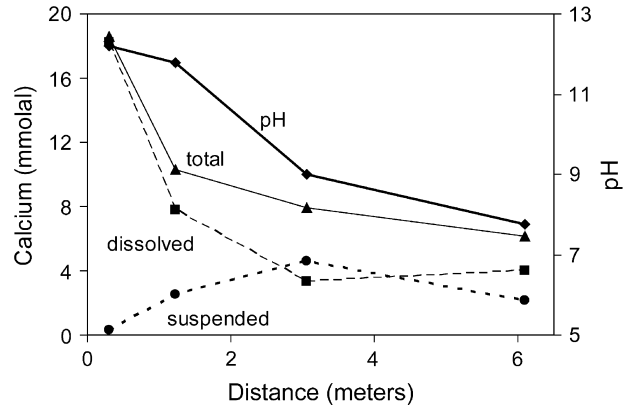


**Figure 6. Variation in calcium concentration and pH along the flowpath from the spring at site 7.**

3.3 mmolal. Calcite precipitation appeared to be occurring throughout the water column, as evidenced by the presence of a significant amount of calcium in the suspended fraction of the samples. A precipitate sample collected 6 m downstream showed a significant accumulation of almost every cation in the analytical suite except Mg, Co, and Sr (Table 1) relative to the precipitate sample collected at the spring. This distribution perhaps reflects the fact that the suspended calcite and iron particles have a collectively large surface area and the longer they are suspended in the water, the more opportunity other metals have to sorb to them, or coprecipitate as the suspended particles grow.

The surface water inflow 1 m downstream from the spring added iron, magnesium, silicon, sulfate, and manganese to the ditch. The iron concentration was higher (100 μmolal) in the surface water than in the spring, but almost all of it was in suspension and it did not dissolve downstream in the ditch. Where the surface runoff mixed with high-pH water from the spring, the dissolved magnesium and silicon concentrations dropped dramatically and there was a corresponding increase in their suspended concentrations, indicating that they flocculated to form suspended material (Figure 7). A geochemical model of this water showed that brucite (Mg(OH)<sub>2</sub>) was supersaturated. The suspended Mg and Si redissolved downstream as the pH decreased.

### Remediation Experiments

Each of the four remediation experiments served to reduce pH in site 3 water at differing rates and to varying extents (Figure 8). In the HCl-addition and the CO<sub>2</sub>-sparging experiments, pH rapidly fell to 7.0. Once this pH was attained, any further addition of HCl and CO<sub>2</sub> was neutralized by the dissolution of the calcite precipitate from site 3 that was added to the flasks prior to the start of the test.

Air sparging also effectively reduced the pH but at a rate ~100 times slower than the CO<sub>2</sub> sparging. Both techniques lower pH by supplying CO<sub>2</sub> to the fluid, but the first uses air, which contains CO<sub>2</sub> at a partial pressure of 10<sup>-3.5</sup> atm, instead of a pure stream of the gas itself. CO<sub>2</sub> cannot accumulate in air-sparged water beyond equilibrium with the atmosphere, so pH in this case cannot drop low enough to dissolve calcite. The experiment

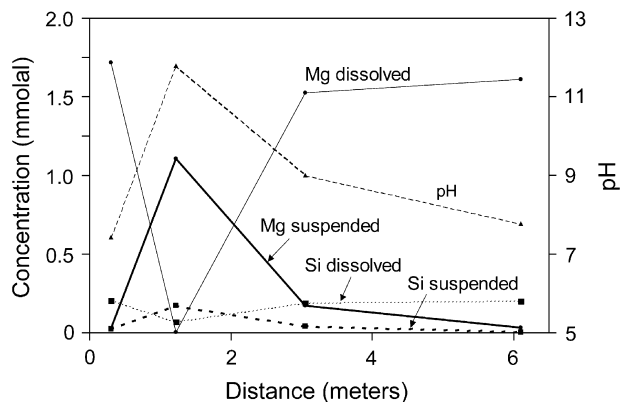


**Figure 7. Variation in magnesium and silicon concentrations along the flowpath from the surface runoff (labeled 0 m) at site 7.**

ended at pH 8.1, a typical value for ground water in contact with calcite.

In the experiment in which dolomite was added, pH fell slowly to 9.1. The reduction was likely due to the dissolution of silica ( $\text{SiO}_2$ ) grains within the crushed aggregate that are more soluble at high pH than neutral pH (Reaction 10). A geochemical model of the experiment showed that of the 35 g of aggregate added to the 1-L flask, only 0.2 g of silica is needed to explain the observed drop in pH. An analogous situation was observed near Wolf Lake in Indiana. Bayless et al. (1998) determined that where ground water flows from slag fill into an underlying sand, silica dissolution causes pH to drop from 12.3 to 9.0.

In evaluating remedial strategies for alkaline sites, it is important to consider the toxicity of the resulting fluid in an aquatic environment. An expensive and maintenance intensive system using acid to neutralize pH, for example, was installed in an alkaline ditch along an elevated highway in Maryland (Broyer 1994). The system succeeded in reducing pH but had little success in lowering the mortality of bioassay organisms (Broyer 2000). At site 3, a bioassay using the Microtox test on the untreated water showed 100% mortality, largely because the

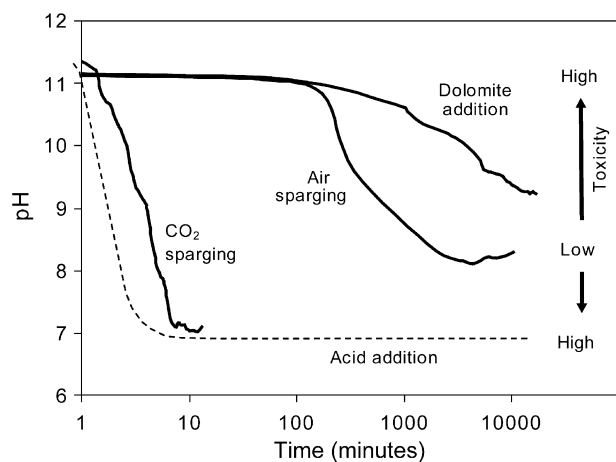


**Figure 8. Variation in pH with time over the course of the four remediation experiments conducted with samples from site 3. Microtox toxicity, shown qualitatively, is at a minimum near pH 8 to 9.**

organisms in the assay are not alkaliphilic. After the pH had been neutralized in the experiments, the toxicity was retested. In the air-sparging experiment, the toxicity had dropped to <10% mortality. The final toxicities of samples from the HCl and  $\text{CO}_2$  experiments were three to four times higher than that of the air-sparging sample. This result is likely due to the release of metals as the calcite sediment dissolved. The long duration of the dolomite-addition experiment prevented the synoptic analysis of a sample for toxicity.

## Conclusions

The results of this study provide new insights into how extremely alkaline ground water is generated, how it redistributes heavy metals, and how it may be remediated. At the sites studied in the Lake Calumet region, calcium silicates in the slag weather to produce a Ca-OH ground water with a pH persistently above 12. This water is buffered by the calcium hydroxide system, which is sensitive to changes in temperature. For this reason, pH at the springs varied considerably throughout the year. The introduction of small amounts of  $\text{CO}_3^{2-}$  to the ground water causes calcite to precipitate; thus, calcite precipitation is limited by the rate of  $\text{CO}_2$  influx from the surface. This behavior contrasts with that of a ground water with near-neutral pH where the addition of  $\text{CO}_2$  causes calcite to dissolve. Where alkaline Ca-OH ground water discharges at springs,  $\text{CO}_2$  is introduced to the water from the atmosphere. Here, layers of calcite up to 20 cm in thickness have formed.

Iron, manganese, and a host of other metals in the metallic portion of the slag have corroded to form oxides and sulfides stable at low temperature. Because redox conditions within the fill vary with position, the iron released during the slag dissolution forms a series of compounds of differing oxidation state, from FeO to  $\text{Fe}_2\text{O}_3$ . Metals like Fe and Mn and the many steel additives, such as Ni and Mo, are insoluble at high pH and do not appear in the ground water in large concentrations. Many of the metals are likely removed from solution by cation substitution and sorption during the formation of  $\text{Fe}_2\text{O}_3$  and other minerals. However, the large amount of metals found in the calcite precipitate at the springs and the total metals analysis for the site 7 water suggest that many metals are mobile in the ground water as particulate matter.

Air sparging appears to be the most effective of the four alternatives considered for remediating the alkaline discharge because it can effectively reduce the toxicity of the water without the danger of dissolving the metal-rich calcite sediment. Because air is free and easy to introduce into the water, this method is also more cost effective than schemes that consume reagents such as  $\text{CO}_2$  or HCl.

## Acknowledgments

This work was supported by U.S. EPA Grant GL985745-01-1 and the Illinois State Water Survey. We thank Michael Machesky, Loretta Skowron, Daniel Webb,

Sofia Lazovsky, and Charles Curtiss of the ISWS for their assistance in the laboratory. We gratefully acknowledge Thomas Johnson, Thomas Anderson, E. Randall Bayless, Chen Zhu, and two anonymous reviewers whose comments greatly improved the manuscript.

**Author's Note:** The authors do not have any conflicts of interest or financial disclosures to report.

**Editor's Note:** The use of brand names in peer-reviewed papers is for identification purposes only and does not constitute endorsement by the authors, their employers, or the National Ground Water Association.

## References

- Azure Environmental, Inc. 2000. <http://www.azureenv.com>.
- Bayless, E.R., T.K. Greeman, and C.C. Harvey. 1998. Hydrology and geochemistry of a slag-affected aquifer and chemical characteristics of slag-affected ground water, northwestern Indiana and northeastern Illinois. USGS Water-Resources Investigations Report 97-4198. Indianapolis, Indiana: USGS.
- Bayless, E.R., and M.S. Schultz. 2003. Mineral precipitation and dissolution at two slag-disposal sites in northwestern Indiana, USA. *Environmental Geology* 45, no. 2: 252–261.
- Berner, U.R. 1988. Modelling the incongruent dissolution of hydrated cement minerals. *Radiochimica Acta* 44/45, no. 2: 387–393.
- Bethke, C.M. 2002. *The Geochemist's Workbench Ver. 4.0*. Urbana, Illinois: University of Illinois.
- Brookins, D.G. 1988. *Eh-pH Diagrams for Geochemistry*. Berlin, Germany: Springer-Verlag.
- Broyer, B.W. 2000. Personal communication, Maryland State Highways Administration, Baltimore.
- Broyer, B.W. 1994. Alkaline leachate and calcareous tufa originating from slag in a highway embankment near Baltimore, Maryland. *Transportation Research Record* 1434, 3–7.
- Colton, C.E. 1985. Industrial wastes in the Calumet Area, 1869–1970. Illinois Hazardous Waste Research and Information Center Research Report 001. Champaign, Illinois: Illinois Hazardous Waste Research and Information Center.
- Cornell, R.M., and U. Schwertmann. 1996. *The Iron Oxides*. Weinheim, Germany: VCH.
- Cravens, S.J., and A.L. Zahn. 1990. Ground-water quality investigation and monitoring program design for the Lake Calumet Area of southeast Chicago. Illinois State Water Survey Contract Report 496. Champaign, Illinois: Illinois State Water Survey.
- Duwelius, R.F., R.T. Kay, and S.T. Prinos. 1996. Ground-water quality in the Calumet Region of northwestern Indiana and northeastern Illinois, June 1993. USGS Water-Resources Investigations Report 95-4244. Indianapolis, Indiana: USGS.
- Fenelon, J.M., and L.R. Watson. 1993. Geohydrology and water quality in the Calumet aquifer in the vicinity of the Grand Calumet River/Indiana Harbor Canal, northwestern Indiana. USGS Water-Resources Investigations Report 92-4115. Indianapolis, Indiana: USGS.
- Hem, J.D. 1985. Study and interpretation of the chemical characteristics of natural water. USGS Water Supply Paper 2254. Reston, Virginia: USGS.
- IEPA. 1986. The southeast Chicago study: An assessment of environmental pollution and public health impacts. Illinois Environmental Protection Agency IEPA/ENV/86-008.
- Kay, R.T., T.K. Greeman, R.F. Duwelius, R.B. King, J.E. Nazimek, and D.M. Petrovski. 1996. Characterization of fill deposits in the Calumet Region of northwestern Indiana and northeastern Illinois. USGS Water-Resources Investigations Report 96-4126. Urbana, Illinois: USGS.
- Khoury, H.N., E. Salameh, and Q. Abdul-Jabar. 1985. Characteristic of an unusual highly alkaline water from the Maqarin area, northern Jordan. *Journal of Hydrology* 81, no. 1–2: 79–91.
- Langmuir, D. 1997. *Aqueous Environmental Geochemistry*. Upper Saddle River, New Jersey: Prentice Hall.
- Lindberg, R.D., and D.D. Runnells. 1984. Groundwater redox reactions: An analysis of equilibrium state applied to Eh measurements and geochemical modeling. *Science* 225, no. 4665: 925–927.
- Mattigod, S.V., D. Rai, L.E. Eary, and C.C. Ainsworth. 1990. Geochemical factors controlling the mobilization of inorganic constituents from fossil fuel combustion residues. *Journal of Environmental Quality* 19, no. 1: 188–201.
- Roadcap, G.S., and W.R. Kelly. 1994. Shallow ground-water chemistry in the Lake Calumet Area, Chicago, Illinois. In *National Symposium on Water Quality*, ed. G.L. Pederson, 253–262. Herndon, Virginia: American Water Resources Association.
- U.S. EPA. 1996. Ecotox thresholds. U.S. EPA ECO update, Intermittent Bulletin vol. 3, no. 2. EPA/540/F-95/038. Washington, DC: U.S. EPA.
- Vythoulkas, G. 1997. Slag materials and their significance on groundwater geochemistry in southeast Chicago. M.S. thesis, University of Illinois at Chicago.
- Zoltai, T., and J.H. Stout. 1984. *Mineralogy*. Minneapolis, Minnesota: Burgess.